Commun. Comput. Phys.
doi: 10.4208/cicp.070313.221113a

Vol. **16**, No. 1, pp. 96-114
July 2014

Immersed Interface CIP for One Dimensional Hyperbolic Equations

Kazufumi Ito[1] and Tomoya Takeuchi[2,3,*]

[1] *Department of Mathematics, North Carolina State University, Raleigh, NC 27695, USA.*
[2] *Collaborative Research Center for Innovative Mathematical Modelling, Institute of Industrial Science, University of Tokyo, Tokyo, Japan.*
[3] *FIRST, Aihara Innovative Mathematical Modelling Project, JST, Kawaguchi, Japan.*

Received 7 March 2013; Accepted (in revised version) 22 November 2013

Communicated by Ming-Chih Lai

Available online 10 April 2014

Abstract. The immersed interface technique is incorporated into CIP method to solve one-dimensional hyperbolic equations with piecewise constant coefficients. The proposed method achieves the third order of accuracy in time and space in the vicinity of the interface where the coefficients have jump discontinuities, which is the same order of accuracy of the standard CIP scheme. Some numerical tests are given to verify the accuracy of the proposed method.

AMS subject classifications: 65M12, 65M25

Key words: CIP method, immersed interface method, hyperbolic equations in discontinuous media.

1 Introduction

In this paper we develop a higher order numerical method for one dimensional hyperbolic equations with discontinuous coefficients, for instance, the scaler advection equation

$$u_t+(c(x)u)_x=0, \quad t>0,\ x\in\mathbb{R}, \tag{1.1}$$

and one dimensional Maxwell's equations

$$\varepsilon(x)E_t=H_x, \quad \mu(x)H_t=E_x, \quad t>0,\ x\in\mathbb{R}. \tag{1.2}$$

*Corresponding author. *Email addresses:* kito@math.ncsu.edu (K. Ito), takeuchi@sat.t.u-tokyo.ac.jp (T. Takeuchi)

The building blocks of the method consist of CIP method and Immersed interface method.

CIP method proposed in [10, 13, 14] approximates the solution to a differential equation through the evolution of more than one degree of freedom per cell, e.g., not only the primitive variable but also its derivatives or other quantities such as the cell average of the solution. The method uses the exact integration for the constant transport equation (the method of characteristics for the constant wave speed) and the time splitting methods for the space varying perturbations, and achieves a higher order of accuracy using a compact stencil. The CIP method has been widely used as an accurate numerical solver for differential equations, which is less-dispersive and less-dissipative than some of the other methods. Here is an incomplete list of references for CIP and related works: nonlinear hyperbolic equations [13], the multi-phase analysis [16], a multi-dimensional the Maxwell's equations [8], light propagation in dielectric media [3], a new mesh system applicable to non-orthogonal coordinate system [15], a numerical investigation of the stability and the accuracy [11]. For the other methods closely related to CIP, we refer to [2, 5].

If the coefficient $c(x)$ has a jump discontinuity, the CIP method without extra care of the discontinuity leads to loss of accuracy. In order to maintain the accuracy in the numerical solution in a neighborhood of the interface, a special treatment should be made. Immersed interface method is one of the technique for the interface problems, which was developed in [6, 17]: A standard numerical method is modified locally near the interface according to the interface relations so that the accuracy in the numerical solution is maintained in the entire domain. For more information, see the monograph [7].

In this article, we develop an immersed interface method for CIP that provides third order accuracy at all grid points, including the adjacent grid to the interface. We construct, by using proper interface conditions, a piecewise Hermite type interpolation on a cell that contains a point of jump discontinuity in $c(x)$.

An outline of our presentation is as follows: Section 2 gives a brief introduction on CIP methods proposed in [13, 14]. Section 3, the main part of the article, is concerned with developing a CIP scheme for discontinuous media. In Section 4 its application to the Maxwell's system is presented. Sections 3 and 4 include some numerical tests to verify the accuracy of the proposed method.

2 Review of CIP

We give a brief review of a CIP method for Eq. (1.1) as a model equation. We first treat the case where the velocity c is a positive constant, and move on to the case of c being a variable velocity.

2.1 CIP for constant velocity

Let us denote the derivative $u_x(t,x)$ by $v(t,x)$. For the constant velocity c, the equations for u and v are

$$u_t+cu_x=0, \quad v_t+cv_x=0.$$

By the method of characteristic, we know that the solution at time $t+\Delta t$ is evaluated by the solution at time t, i.e., $u(t+\Delta t,x)=u(t,x-c\Delta t)$ and $v(t+\Delta t,x)=v(t,x-c\Delta t)$ for arbitrary t, $\Delta t>0$ and x.

Suppose the function values and the derivatives, u^n and v^n, are given at all grid points x_k, $k\in\mathbb{N}$ which are not necessarily uniform. The superscript n indicates that these values are defined at time $t=t_n$. For any grid point x_k, there exits unique grid point x_j such that the upwind point $y_k:=x_k-c\Delta t$ is included in the interval $[x_{j-1},x_j]$. We denote the subscript of such grid point by $j(k)$. The profile inside the interval $[x_{j(k)-1},x_{j(k)}]$ can be interpolated by a cubic polynomial $H(x)$ defined using values $u^n_{j(k)-1},v^n_{j(k)-1},u^n_{j(k)},v^n_{j(k)}$ at two end points, and thus the approximations u^{n+1}_k to $u(t^n+\Delta t,x)$ and v^{n+1}_k to $v(t^n+\Delta t,x)$ are given by

$$u^{n+1}_k=H(y_k), \quad v^{n+1}_k=H_x(y_k). \tag{2.1}$$

Here, the cubic interpolation polynomial H is defined by the condition

$$H(x_{j(k)-1})=u^n_{j(k)-1}, \quad H_x(x_{j(k)-1})=v^n_{j(k)-1}, \quad H(x_{j(k)})=u^n_{j(k)}, \quad H_x(x_{j(k)})=v^n_{j(k)},$$

and H and H_x are given by (cf. [10])

$$H(x)=a(x-x_{j(k)-1})^3+b(x-x_{j(k)-1})^2+v^n_{j(k)-1}(x-x_{j(k)-1})+u^n_{j(k)-1}, \tag{2.2a}$$
$$H_x(x)=3a(x-x_{j(k)-1})^2+2b(x-x_{j(k)-1})+v^n_{j(k)-1}, \tag{2.2b}$$

where

$$a=\frac{(v^n_{j(k)}+v^n_{j(k)-1})\Delta x-2(u^n_{j(k)}-u^n_{j(k)-1})}{\Delta x^3}, \quad b=\frac{3(u^n_{j(k)}-u^n_{j(k)-1})-(v^n_{j(k)}+2v^n_{j(k)-1})\Delta x}{\Delta x^2},$$
$$\Delta x=x_{j(k)}-x_{j(k)-1}.$$

Let $\lambda:=\frac{x_{j(k)}-y_k}{x_{j(k)}-x_{j(k)-1}}$. Obviously $0\le\lambda\le 1$. The one step map (2.1) is written more explicitly;

$$u^{n+1}_k=a_1u^n_{j(k)}+\Delta x\,a_2v^n_{j(k)}+b_1u^n_{j(k)-1}+\Delta x\,b_2v^n_{j(k)-1}, \tag{2.3a}$$
$$v^{n+1}_k=a_3u^n_{j(k)}+\Delta x\,a_4v^n_{j(k)}+b_3u^n_{j(k)-1}+\Delta x\,b_4v^n_{j(k)-1}, \tag{2.3b}$$

where

$$a_1=(1-\lambda)^2(1+2\lambda), \quad a_2=-(1-\lambda)^2\lambda, \quad a_3=6\lambda(1-\lambda), \quad a_4=(1-\lambda)(1-3\lambda),$$
$$b_1=\lambda^2(3-2\lambda), \quad b_2=(1-\lambda)(1-3\lambda), \quad b_3=-6\lambda(1-\lambda), \quad b_4=(3\lambda-2)\lambda.$$

Remark 2.1. The cubic interpolation is one of the possible choice in CIP methods, indeed, higher order polynomials are used to derive a more accurate CIP scheme: For instance, the fifth order interpolation polynomial H can be used in CIP scheme by introducing the second order derivative $w := u_{xx}$ as unknown variable. If the velocity is constant the CIP scheme becomes

$$u_k^{n+1} = H(y_k), \quad v_k^{n+1} = H_x(y_k), \quad w_k^{n+1} = H_{xx}(y_k).$$

It is reported in [11] that the CIP scheme with the fifth order polynomial is fourth order in function value.

2.2 CIP for variable velocity

Let $c > 0$ in (1.1) be a smooth function. The CIP method proposed in [15] solves Eq. (1.1) in the following way. The detail can be found in the article.

The equation (1.1) is transformed into a non-conservative form,

$$u_t + c(x)u_x = -c_x(x)u,$$

and the equation for $v = u_x$ is derived by differentiating the equation with respect to x:

$$v_t + c(x)v_x = -c_{x,x}(x)u - 2c_x(x)v.$$

These equations are split into the advection phase and the non-advection phase:

$$\begin{array}{lll} \text{advection phase:} & u_t + c(x)u_x = 0, & v_t + c(x)v_x = 0, \\ \text{non-advection phase:} & u_t = -c_x(x)u, & v_t = -c_{x,x}(x)u - 2c_x(x)v. \end{array} \tag{2.4}$$

The former equations are solved using CIP (2.1) with the choice of $y_k = x_k - c^*\Delta t$ where the freezed velocity defined by $c^* = \frac{c(x_k)+c(x_k - c(x_k)\Delta t)}{2}$ is used in each interval. The latter equations are solved by employing an exponential finite difference method where the freezed velocity $c_x(y_k)$ and $c_{xx}(y_k)$ are used. We note that the splitting procedure does not allow us to take an arbitrary CFL number, i.e., the time step is restricted by $\max_x c(x)\Delta t \le \min_k(x_k - x_{k-1})$. It is reported in [15] that the present scheme is the third order in time and space in function value, and that the scheme becomes first order with other choice of the upwind point y_k such as $y_k = -c(x_k)\Delta t$ and $y_k = -c(x_k - c(x_k)\Delta t)\Delta t$. Theoretical justification to support for the splitting procedure to work has not been presented.

2.3 Exact time integration CIP for variable velocity

Based entirely on the characteristic method, one can derive a variant of CIP scheme in which no splitting procedure such as (2.4) is required even when the velocity is not constant. The method has several advantages: It has no CFL limitation for a variable coefficient, and can be extended to equations in higher dimension with variable coefficients.

We first consider the advection equation (1.1) with sufficiently smooth $c(x)$ as a model equation. Let u be the exact solution of the equation, and let $\xi(s;x)$ denote the solution of the characteristic equation to (1.1), i.e.,

$$\frac{d\xi(s;x)}{ds}=c(\xi(s;x)),\quad \xi(t+\Delta t;x)=x, \tag{2.5}$$

We shall use the sensitivity of $\xi(s;x)$ with respect to x,

$$\frac{\partial\xi(s;x)}{\partial x}=\frac{c(x)}{c(\xi(s;x))}.$$

Let $y(x):=\xi(t;x)$ be the upwind point. Then the solution value at x and at time $t+\Delta t$ is given by the solution value at $y(x)$ at time t (see [4]):

$$u(x,t+\Delta t)=\frac{c(y(x))}{c(x)}u(y(x),t). \tag{2.6}$$

The derivative $u_x(t+\Delta t,x)$ is obtained by differentiating (2.6) with respect to x:

$$\begin{aligned}u_x(t+\Delta t,x)&=\frac{c'(y)y'c(x)-c(y)c'(x)}{c^2(x)}u(y,t)+\frac{c(y)}{c(x)}u_x(y,t)y'\\&=\left(\frac{c'(y)}{c(x)}-\frac{c'(x)}{c(x)}\right)\frac{c(y)}{c(x)}u(y,t)+\left(\frac{c(y)}{c(x)}\right)^2u(y,t).\end{aligned}$$

Here we used the sensitivity of the upwind point $y(x)=\xi(t;x)$ with respect to x, i.e.,

$$\frac{dy(x)}{dx}=\frac{c(x)}{c(y(x))}.$$

We discretize the time domain and the spatial domain with grid size $\Delta t>0$ and $\Delta x_k=x_k-x_{k-1}$, $k\in\mathbb{Z}$. The mesh size is not necessarily uniform. Write $t_n=n\Delta t$, $n\in\mathbb{N}$. Let us denote the numerical solution for $u(t_n,x_k)$ and $u_x(t_n,x_k)$ by u_k^n and v_k^n respectively for $k\in\mathbb{N}$. Let $y_k:=\xi(t;x_k)$ and $j(k)\in\mathbb{N}$ such that $y_k\in[x_{j(k)-1},x_{j(k)}]$. We obtain the CIP scheme

$$u_k^{n+1}=\frac{c(y_k)}{c(x_k)}H(y_k),\quad v_k^{n+1}=\frac{c(y_k)}{c(x_k)}\left[\frac{c'(y_k)}{c(x_k)}-\frac{c'(x_k)}{c(x_k)}\right]H(y_k)+\left(\frac{c(y_k)}{c(x_k)}\right)^2H_x(y_k), \tag{2.7}$$

where H denotes the cubic interpolation (2.2). The cubic polynomial H is referred to as *cubic interpolation profile* or *constrained interpolation profile* in existing articles, and in this paper we use the term *cubic interpolation profile*. In summary, CIP scheme for (1.1) is composed of

CIP0 Solve the characteristic ODE (2.5) subject to $\xi(t+\Delta t)=x_k$ to find the upwind point $y_k=\xi(t,x_k)$.

CIP1 For each time level t_n, construct the cubic interpolation profile $H(x)$ by (2.2).

CIP2 Update u_k^{n+1} and v_k^{n+1} by (2.7).

Similar argument leads to the exact time integration formula for the transport equation $u_t+c(x)u_x=0$: For the cubic Hermite interpolation CIP, we have

$$u_k^{n+1}=H(y_k), \quad v_k^{n+1}=\frac{c(y_k)}{c(x_k)}H_x(y_k).$$

And for the fifth order polynomial interpolation CIP, we have

$$\begin{aligned} u_k^{n+1}&=H(y_k), \quad v_k^{n+1}=\frac{c(y_k)}{c(x_k)}H_x(y_k), \\ w_k^{n+1}&=\frac{c(y_k)}{c(x_k)}\left[\frac{c'(y_k)}{c(x_k)}-\frac{c'(x_k)}{c(x_k)}\right]H_x(y_k)+\left(\frac{c(y_k)}{c(x_k)}\right)^2 H_{xx}(y_k). \end{aligned}$$

3 Immersed interface method for CIP

This section is the main part of the article. We develop the immersed interface method for CIP (IIM-CIP for short) for transport equations with discontinues coefficient;

$$u_t+cu_x=0, \quad t>0, \ x\in\mathbb{R}, \qquad u(0,x)=u_0(x), \ x\in\mathbb{R}, \tag{3.1}$$

where $c>0$ is a piecewise smooth that has a jump across $x=\alpha$. That is, $c=c^-$ in $x<\alpha$ and $c=c^+$ in $x>\alpha$ with $c^-\neq c^+$. We first consider the case where the interface falls in an interval, and then we consider the case where the interface coincides with a grid point.

Case 1. Interface falls in an interval.

We assume that the interface falls in an interval (x_{j-1},x_j). We call the interval $[x_{j-1},x_j]$ *an irregular interval* or *an irregular cell*, and the point x_j *an irregular point*. The interface condition on u is imposed according to the physical phenomena under consideration. We take $[u]=0$ as an interface condition at the interface α, where $[u]:=\lim_{x\to\alpha^+}u^+(x)-\lim_{x\to\alpha^-}u^-(x)$. Here $u^-(x)=u(x)|_{[x_{j-1},\alpha]}$ and $u^+(x)=u(x)|_{[\alpha,x_j]}$. The treatment of an interface condition $[cu]=0$ will be briefly discussed at the end of this section.

From the interface condition coupled with the equation, we know the flux $(cu)_x=cu_x$ is also continuous across the interface, and thus the derivative u_x has a jump discontinuity at the interface. Because of the discontinuity in u_x, the standard CIP using a single profile in an interval will not provide an accurate solution.

In stead of using a single interpolation, we use a piecewise interpolation polynomial to approximate the solution $u(t_n,x)$ in the interval. We consider Hermite cubic polynomial for the approximation. The discussion below can be extended to any order polynomial interpolations.

Firstly, we derive a time integration formula for the exact solution and its derivative, and then we propose a numerical scheme (IIM-CIP scheme) to update the numerical solution u_j^n and the derivative v_j^n to the next time level.

Piecewise cubic polynomial. The interface condition $[u]=0$ coupled with Eq. (3.1) yields the relations $[c^k\frac{\partial^k u}{\partial x^k}]=0$, $k\in\mathbb{N}$. See [17] for the derivation. Obviously, it is impossible to construct a single polynomial interpolation that satisfies the relations. We introduce two polynomials of the form $H^{\pm}(x)=\sum_{k=0}^{3}\frac{a_k^{\pm}}{k!}(x-\alpha)^k$. We determine the eight unknowns via the interface relations and the interpolation conditions:

$$\begin{cases} H^-(\alpha)=H^+(\alpha), & c^-H_x^-(\alpha)=c^+H_x^+(\alpha), \\ (c^-)^2H_{xx}^-(\alpha)=(c^+)^2H_{xx}^+(\alpha), & (c^-)^3H_{xxx}^-(\alpha)=(c^+)^3H_{xxx}^+(\alpha), \end{cases} \tag{3.2}$$

$$H^-(x_{j-1})=u_{j-1}^n,\quad H_x^-(x_{j-1})=v_{j-1}^n,\quad H^+(x_j)=u_j^n,\quad H_x^+(x_j)=v_j^n. \tag{3.3}$$

The first equations yield

$$a_0^-=a_0^+,\quad c^-a_1^-=c^+a_1^+,\quad (c^-)^2a_2^-=(c^+)^2a_2^+,\quad (c^-)^3a_3^-=(c^+)^3a_3^+, \tag{3.4}$$

and thus, introducing new parameters $a=(a_0,\cdots,a_3)^\top$, we can write $H^{\pm}(x)=\sum_{\ell=0}^{3}\frac{a_\ell}{\ell!}\left(\frac{x-\alpha}{c^{\pm}\Delta x}\right)^\ell$. Then using the interpolation conditions (3.3), we obtain the system $Aa=f$, where

$$A=\begin{pmatrix} 1 & \frac{\theta}{c^+} & \frac{\theta^2}{2(c^+)^2} & \frac{\theta^3}{3!(c^+)^3} \\ 0 & \frac{1}{c^+} & \frac{\theta}{(c^+)^2} & \frac{\theta^2}{2(c^+)^3} \\ 1 & \frac{(\theta-1)}{c^-} & \frac{(\theta-1)^2}{2(c^-)^2} & \frac{(\theta-1)^3}{3!(c^-)^3} \\ 0 & \frac{1}{c^-} & \frac{(\theta-1)}{(c^-)^2} & \frac{(\theta-1)^2}{2(c^-)^3} \end{pmatrix},\quad f=\begin{pmatrix} u_j^n \\ \Delta x v_j^n \\ u_{j-1}^n \\ \Delta x v_{j-1}^n \end{pmatrix},$$

and $\theta=\frac{x_j-\alpha}{\Delta x}$. The inverse A^{-1} is given as $A^{-1}=BC$ where B and C are defined by

$$B=\begin{pmatrix} \phi^2(3\theta c^-+\phi c^+) & -\theta\phi^2 & \theta^2(\theta c^-+3\phi c^+) & \theta^2\phi \\ 6\theta\phi(c^-)^2 & \phi(\phi c^+-2\theta c^-) & -6\theta\phi(c^+)^2 & \theta(\theta c^- -2\phi c^+) \\ 6(c^-)^2(\theta c^- -\phi c^+) & -2c^-(\theta c^- -2\phi c^+) & 6(c^+)^2(\phi c^+ -\theta c^-) & 2c^+(\phi c^+ -2\theta c^-) \\ -12(c^-)^3c^+ & 6(c^-)^2c^+ & 12c^-(c^+)^3 & 6c^-(c^+)^2 \end{pmatrix},$$

$$C=\mathrm{diag}\big((c^+)^2c^3,(c^+)^2c^2,(c^-)^2c^3,(c^-)^2c^2\big)\quad \text{with } c=\left(\theta c^-+\phi c^+\right)^{-1},$$

where $\phi=1-\theta$. The coefficient a is uniquely determined by $a=A^{-1}f$. We define a piecewise polynomial $H(x)$ on $[x_{j-1},x_j]$ by $H|_{[x_{j-1},\alpha]}=H^-|_{[x_{j-1},\alpha]}$, $H|_{[\alpha,x_j]}=H^+|_{[\alpha,x_j]}$ and call it *the immersed interface cubic profile* to the data set f. The piecewise polynomial is also denoted by $H^{\pm}$.

Fig. 1(a) illustrates the immersed interface cubic profile $H^{\pm}(x)$ on the interval $[x_{j-1},x_j]$. One can see that the profile is continuous at the interface but has discontinuity in the one-sided derivative at the point.

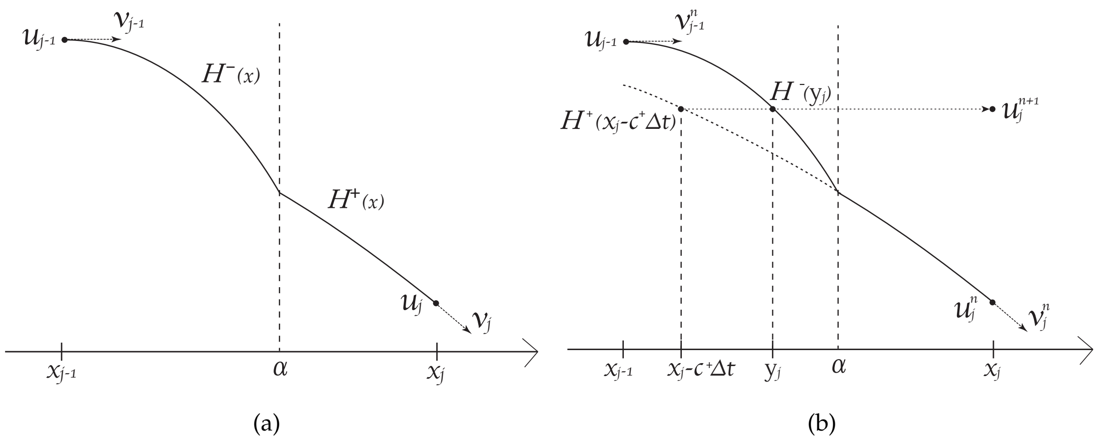

Figure 1: (a) The piecewise cubic polynomial $H^{\pm}$ on the irregular interval. It is continuous at the interface α and has a jump discontinuity in the one-sided derivative at the interface. (b) Graphical illustration of the IIM-CIP scheme. We update u_j^{n+1} and v_j^{n+1} at the time level t_{n+1} at the grid x_j with using the value $H^{+}(x_j-c^{+}\Delta t)$ and its derivative $H_x^{+}(x_j-c^{+}\Delta t)$.

Let us investigate the accuracy of the immersed interface cubic profile: We consider the immersed interface cubic profile $H^{\pm}(x)$ to the exact solution $u(t_n,x)$. From the interface relations (3.2), the polynomials H^{+} and H^{-} can be written in the form $H^{+}(x)=\sum_{\ell=0}^{3}\frac{a_\ell}{\ell!}\left(\frac{x-\alpha}{c^{+}\Delta x}\right)^{\ell}$ and $H^{-}(x)=\sum_{\ell=0}^{3}\frac{a_\ell}{\ell!}\left(\frac{x-\alpha}{c^{-}\Delta x}\right)^{\ell}$. The interpolation condition with exact solution as a data set,

$$H^{-}(x_{j-1})=u(t_n,x_{j-1}),\quad H_x^{-}(x_{j-1})=u_x(t_n,x_{j-1}),\quad H^{+}(x_j)=u(t_n,x_j),\quad H_x^{+}(x_j)=u_x(t_n,x_j),$$

leads to the system $Aa=f$ for the coefficient a, where

$$f=(u^{+}(t_n,x_j),\Delta x\, u_x^{+}(t_n,x),u^{-}(t_n,x_{j-1}),\Delta x\, u_x^{-}(t_n,x))^{\top}.$$

Theorem 3.1 (Accuracy of the immersed interface cubic profile). *Let $u(t,x)$ be the solution of* (3.1). *We have the following error estimates*

$$u(t_n,x)-H(x)=\mathcal{O}((\Delta x)^4),\quad u_x(t_n,x)-H_x(x)=\mathcal{O}((\Delta x)^3),\quad x\in[x_{j-1},x_j].$$

Here the one-sided derivative is taken at the interface α.

Proof. The Taylor expansion for $u^{\pm}(t_n,x)$ at the interface α and the interface relations

$$\begin{aligned}&u^{-}(t_n,\alpha)=u^{+}(t_n,\alpha),\quad c^{-}u_x^{-}(t_n,\alpha)=c^{+}u_x^{+}(t_n,\alpha),\\&(c^{-})^2u_{xx}^{-}(t_n,\alpha)=(c^{+})^2u_{xx}^{+}(t_n,\alpha),\quad (c^{-})^3u_{xxx}^{-}(t_n,\alpha)=(c^{+})^3u_{xxx}^{+}(t_n,\alpha),\end{aligned}$$

lead to

$$
\begin{aligned}
u^+(t_n,x_j) &= b_0+b_1\frac{\theta}{c^+}+\frac{b_2}{2}\left(\frac{\theta}{c^+}\right)^2+\frac{b_3}{3!}\left(\frac{\theta}{c^+}\right)^3+\mathcal{O}((\Delta x)^4),\\
\Delta x\, u_x^+(t_n,x) &= \frac{b_1}{c^+}+b_2\frac{\theta}{(c^+)^2}+\frac{b_3}{2}\frac{\theta^2}{(c^+)^3}+\mathcal{O}((\Delta x)^4),\\
u^-(t_n,x_{j-1}) &= b_0+b_1\frac{\theta-1}{c^-}+\frac{b_2}{2}\left(\frac{\theta-1}{c^-}\right)^2+\frac{b_3}{3!}\left(\frac{\theta-1}{c^-}\right)^3+\mathcal{O}((\Delta x)^4),\\
\Delta x\, u_x^-(t_n,x) &= \frac{b_1}{c^-}+b_2\frac{\theta-1}{(c^-)^2}+\frac{b_3}{2}\frac{(\theta-1)^2}{(c^-)^3}+\mathcal{O}((\Delta x)^4),
\end{aligned}
$$

where $b_0=u^+(t_n,\alpha)$, $b_1=c^+u_x^+(t_n,\alpha)$, $b_2=(c^+)^2u_{xx}^+(t_n,\alpha)$ and $b_3=(c^+)^3u_{xxx}^+(t_n,\alpha)$. Thus we have $A(a-b)=(r_1,r_2,r_3,r_4)^\top$ where $r_i=\mathcal{O}((\Delta x)^4)$ for $i=1,2,3,4$. Since the components of $A^{-1}=BC$ is of order $\mathcal{O}(1)$, we have that $a_k-b_k=\mathcal{O}((\Delta x)^4)$ for $k=0,1,2,3$. Thus we obtain the desired estimates. $\square$

Update formula. Now that we have constructed the immersed interface cubic profile in the irregular interval, we attempt to build an update formula for numerical solutions with the aid of the method of characteristic. We assume that $\Delta t>0$ is taken sufficiently small so that CFL number is less than 1, i.e., $c^\pm\Delta t<\Delta x$. Therefore y_k is always included in the interval (x_{k-1},x_k) for all k.

If x_j is an regular point, the numerical solution is updated by (2.3) with $\lambda=\frac{c^-\Delta t}{\Delta x}$ or $\lambda=\frac{c^+\Delta t}{\Delta x}$ depending on the velocity at the grid $x=x_j$. Let us assume that x_j is an irregular grid, and let us consider the characteristic curve $x=x(s)$ with $x(\Delta t)=x_j$. Let us denote the upwind point $x(0)$ by y_j.

Proposition 3.1. Suppose that there exists an interface in the interval $[x_{j-1},x_j]$. If $\alpha\le x_j-c^+\Delta t$,

$$
\begin{aligned}
&y_j=x_j-c^+\Delta t,\\
&u^+(t_{n+1},x_j)=u^+(t_n,y_j),\quad u_x^+(t_{n+1},x_j)=u_x^+(t_n,y_j).
\end{aligned}
$$

If $x_j-c^+\Delta t\le\alpha$,

$$
\begin{aligned}
&y_j=\alpha+\frac{c^-}{c^+}(x_j-\alpha)-c^-\Delta t,\\
&u^+(t_{n+1},x_j)=u^-(t_n,y_j),\quad u_x^+(t_{n+1},x_j)=\frac{c^-}{c^+}u_x^-(t_n,y_j).
\end{aligned}
$$

Proof. Let us assume that $\alpha\le x_j-c^+\Delta t$. The characteristic ODE (2.5) become $\dot{x}(s)=c^+$, and thus we have $y_j=x_j-c^+\Delta t$, $u^+(t_{n+1},x_j)=u^+(t_n,x_j-c^+\Delta t)$ and $u_x^+(t_{n+1},x_j)=u_x^+(t_n,x_j-c^+\Delta t)$.

Next let us assume that $x_j - c^+\Delta t \le \alpha$. There exists $s^* > 0$ such that $\alpha = x(s^*)$. The characteristic curve obeys

$$\dot{x}(s) = c^- \quad (0 \le s \le s^*), \quad \dot{x}(s) = c^+ \quad (s^* \le s \le \Delta t).$$

It is obvious to see that $\alpha - y_j = c^- s^*$, $x_j - \alpha = c^+(\Delta t - s^*)$, which yields $y_j = \alpha + \frac{c^-}{c^+}(x_j - \alpha) - c^-\Delta t$, $s^* = \Delta t - \frac{x_j - \alpha}{c^+}$. The characteristic ODE for $z(s) = u(s,x(s))$ becomes $\frac{d}{ds}u^-(s,x(s)) = 0$ $(0 \le s \le s^*)$ and $\frac{d}{ds}u^+(s,x(s)) = 0$ $(s^* \le s \le \Delta t)$. Using the interface condition $[u] = 0$, it follows $u^+(t_{n+1},x_j) = u^+(s^*,\alpha) = u^-(s^*,\alpha) = u^-(t_n,y_j)$. Similarly, with the characteristic ODE for $u_x(s,x(s))$ and the relation $[cu_x] = 0$, we obtain $u_x^+(t_{n+1},x_j) = u_x^+(s^*,\alpha) = \frac{c^-}{c^+}u_x^-(s^*,\alpha) = \frac{c^-}{c^+}u_x^-(t_n,y_j)$. $\square$

Thus we arrive at a CIP scheme for Eq. (3.1): Let H^+ and H^- be cubic polynomials defined by (3.2) and (3.3). If $\alpha \le x_j - c^+\Delta t$,

$$u_j^{n+1} = H^+(x_j - c^+\Delta t), \quad v_j^{n+1} = H_x^+(x_j - c^+\Delta t). \tag{3.5}$$

And, if $x_j - c^+\Delta t \le \alpha$,

$$u_j^{n+1} = H^-(y_j), \quad v_j^{n+1} = \frac{c^-}{c^+}H_x^-(y_j). \tag{3.6}$$

where $y_j = \alpha + \frac{c^-}{c^+}(x_j - \alpha) - c^-\Delta t$.

It seems one must appropriately choose either (3.5) or (3.6) according to the condition $\alpha \le x_j - c^+\Delta t$ or $x_j - c^+\Delta t \le \alpha$. However, we can avoid this treatment, and the update scheme at the irregular point is solely based on (3.5). One can show that if $x_j - c^+\Delta t \le \alpha$, the numerical solution is also given by (3.5), i.e.,

$$u^{n+1} = H^-(y_j) = H^+(x_j - c^+\Delta t), \quad v^{n+1} = \frac{c^-}{c^+}H_x^-(y_j) = H_x^+(x_j - c^+\Delta t). \tag{3.7}$$

Indeed, from $\frac{c^+}{c^-}(y_j - \alpha) = x_j - c^+\Delta t - \alpha$ and (3.4), we have

$$\begin{aligned} a_\ell^-(y_j - \alpha)^\ell &= a_\ell^+\left(\frac{c^+}{c^-}\right)^\ell (y_j - \alpha)^\ell = a_\ell^+(x_j - c^+\Delta t - \alpha)^\ell, \\ \frac{c^-}{c^+}a_\ell^-(y_j - \alpha)^{\ell-1} &= a_\ell^+\left(\frac{c^+}{c^-}\right)^{\ell-1}(y_j - \alpha)^{\ell-1} = a_\ell^+(x_j - c^+\Delta t - \alpha)^{\ell-1}, \end{aligned}$$

which implies (3.7).

Fig. 1(b) illustrates that how $H^+(x_j - c^+\Delta t)$ correctly updates the function value and its derivative u_j^{n+1} and v_j^{n+1} at the irregular grid even when $x_j - c^+\Delta t \le \alpha$. The update (3.6) is not necessary for the computation of the numerical solution.

Here is the summary of the IIM-CIP.

IIM-CIP1 Construct the cubic profile on each interval. If the interval is irregular, then construct the immersed interface cubic profile.

IIM-CIP2 Update u_j^{n+1} and v_j^{n+1}: If x_j is a regular grid, use (2.3) with $\lambda=\frac{c\Delta t}{\Delta x}$ where $c=c^-$ if $x_j<\alpha$ or $c=c^+$ if $\alpha<x_j$. If x_j is the irregular grid, use (3.5).

It is worth pointing out that if c is a continuous constant, then $H^+(x)=H^-(x)$ by (3.4), and thus the profile $H(x)$ is identical to the cubic interpolated polynomial.

Let us consider the advection equation $u_t-(cu)_x=0$, with $c>0$. Assume that an interface locates $x=\alpha\in[x_{j-1},x_j]$. Then x_{j-1} is an irregular point and the numerical solutions at x_{j-1} are give by

$$u_{j-1}^{n+1}=H^-(x_{j-1}+c^-\Delta t),\quad v_{j-1}^{n+1}=H_x^-(x_{j-1}+c^-\Delta t).$$

Interface condition $[cu]=0$. The interface condition yields to the interface relations $[c^i\frac{\partial^i u}{\partial x^i}]=0$, $i\in\mathbb{N}$. We define the immersed interface polynomial $H^\pm$ using the conditions

$$[cu]=0,\quad [c^2u_x]=0,\quad [c^3u_{xx}]=0,\quad [c^4u_{xxx}]=0,$$

and the interpolation condition (3.3). The numerical solutions are given by the same form as

$$u_j^{n+1}=H^+(x_j-c^+\Delta t),\quad v_j^{n+1}=H_x^+(x_j-c^+\Delta t).$$

Case 2. The interface locates on a grid point.

So far we have assumed that the interface does not coincide with any grid points, i.e, $\alpha\neq x_k$ for all $k\in\mathbb{N}$. Here we consider the case $\alpha=x_k$ for a grid x_k. The treatment of the case is much simpler than the approach discussed so far. Let us consider the case $[u]=0$. Then at the interface we have

$$u^-(x_k)=u^+(x_k),\quad c^-u_x^-(x_k)=c^+u_x^+(x_k).$$

The last equation suggests that we should introduce a flux $\hat{v}_k:=c^-u_x^-=c^+u_x^+$ as a new variable at the grid x_k. Now the unknown quantities at the grid x_k are the function value u_k and the flux $\hat{v}_k$. The one-sided derivatives $u_x^\pm$ at the gird are given by $u_x^\pm(x_k)=\frac{\hat{v}_k}{c^\pm}$. The cubic interpolation in the interval $[x_{k-1},x_k]$ is defined by

$$H(x_{k-1})=u_{k-1},\quad H_x(x_{k-1})=v_{k-1},\quad H(x_k)=u_k,\quad H_x(x_k)=\frac{\hat{v}_k}{c^-},$$

and the numerical solutions of the next time step u_k^{n+1} and $\hat{v}_k^{n+1}$ are given by

$$u_k^{n+1}=H(x_k-c^-\Delta t),\quad \hat{v}_k^{n+1}=c^-H_x(x_k-c^-\Delta t).$$

On the other hand, the cubic interpolation in the interval $[x_k,x_{k+1}]$ is defined by

$$H(x_k)=u_k,\quad H_x(x_k)=\frac{\hat{v}_k}{c^+},\quad H(x_{k+1})=u_{k+1},\quad H_x(x_{k+1})=v_{k+1},$$

and u_{k+1}^{n+1} and v_{k+1}^{n+1} are given by the usual way.

As for the interface condition $[cu]=0$, we introduce $\hat{u}_k := c^- u^- = c^+ u^+$ and $\hat{v}_k := (c^-)^2 u_x^- = (c^+)^2 u_x^+$ as new variables at the grid $x = x_k$, and define the cubic interpolation in the interval $[x_{k-1}, x_k]$ by

$$H(x_{k-1}) = u_{k-1}, \quad H_x(x_{k-1}) = v_{k-1}, \quad H(x_k) = \frac{\hat{u}_k}{c^-}, \quad H_x(x_k) = \frac{\hat{v}_k}{(c^-)^2}.$$

We update $\hat{u}_k^{n+1}$ and $\hat{v}_k^{n+1}$ by

$$\hat{u}_k^{n+1} = c^- H(x_k - c^- \Delta t), \quad \hat{v}_k^{n+1} = (c^-)^2 H_x(x_k - c^- \Delta t).$$

We list up the features and the advantages of IIM-CIP:

(i) The method becomes the standard CIP if the discontinuities in the coefficients disappear.

(ii) The structure of the IIM-CIP is as simple as CIP: The cubic interpolation profile H is replaced by the immersed interface cubic profile.

(iii) The immersed interface cubic profile is an interpolation for the solution on the irregular cell, and the third order of accuracy in time and space is achieved in a vicinity of the interface, which is the same order of accuracy of the standard CIP scheme for $CFL < 1$.

(iv) No grid refinement is required to maintain the accuracy in a vicinity of the interface.

3.1 Numerical results

In this section we present some numerical results to illustrate IIM-CIP for discontinuous velocity and verify third order accuracy in time and space.

Example 3.1. We consider the transport equation (3.1) with discontinuity

$$c(x) = \begin{cases} c_1, & 0 \le x \le \alpha, \\ c_2, & \alpha \le x \le 1. \end{cases}$$

Both of the interface condition $[u]=0$ and $[cu]=0$ at the interface $x=\alpha$ are considered. We apply the IIM-CIP method developed in Section 3. The exact solution for $[u]=0$ is given by $u(t,x) = u(0,y)$, where

$$y = \begin{cases} x - c_2 t, & \text{if } x \ge \alpha \text{ and } t \le \frac{x-\alpha}{c_2}, \\ x - c_1 t, & \text{if } x \le \alpha, \\ \frac{c_1}{c_2}(x - c_2 t) + (1 - \frac{c_1}{c_2})\alpha, & \text{otherwise .} \end{cases}$$

The exact solution for $[cu]=0$ is $u(t,x)=\frac{c(y)}{c(x)}u(0,y)$.

In the numerical experiments, the spatial domain $[0,1]$ is uniformly discretized with mesh size $\Delta x=\frac{1}{N}$ for $N\in\{100,200,400,800\}$, and the time step size is $\Delta t=0.25\Delta x$. The location of the interface is set to be $\alpha=0.5+\frac{\sqrt{2}}{100}\sim 5.1414$ so that α falls in an interval for all N. The velocity is set to be $c_1=2$ and $c_2=1$. The initial condition for the numerical solution $\{u_k^0\}_k^N$ is given by $u_k^0=u(0,x_k)$, where $u(0,x)=\exp(-\frac{(x-0.2)^2}{0.05^2})$. And $\{v_k^0\}_k^N$ is computed by central finite difference of $\{u_k^0\}_k^N$. For each mesh size, the error in the numerical solutions at time $t=0.5$ is measured by

$$\epsilon(u^n):=|u^n-U^n|_{\ell^\infty},\quad \epsilon(v^n):=|v^n-V^n|_{\ell^\infty}, \tag{3.8}$$

where $u^n=\{u_k^n\}_{k=1}^N$ and $v^n=\{v_k^n\}_{k=1}^N$ are the numerical solutions, and $U^n=\{u(t^n,x_k)\}_{k=1}^N$ are the grid values of the exact solution and $V^n=\{u_x(t^n,x_k)\}_{k=1}^N$ are the grid values of its derivative at $t^n=0.5$.

Plots of Fig. 3 show numerical solutions (dot) and exact solutions (solid line) at time $t=0.14$ (left), $t=0.17$ (center) and $t=0.25$ (right) to the transport equation with the jump condition $[u]=0$ at α. The mesh size $\frac{1}{200}$ is used to compute the numerical solutions. The vertical solid line indicates the location of the interface. As the wave passes the interface, it slows down and becomes narrower. No spurious oscillation is observed in the numerical solutions.

Numerical solutions and the exact solution for the interface condition $[cu]$ is plotted in Fig. 4. The exact solution u has a jump discontinuity at the interface. We see that the numerical solution also exhibits the distinct jump at the interface. A magnification of the figure at time $t=0.14$ around the interface is depicted in Fig. 5 so that the jump discontinuity in the numerical solution and the exact solution are more visible. We can see that the numerical solution almost coincides with the exact solution.

Plots of Fig. 2 and Table 1 show the error in the computed solutions at $t=0.5$ against the number of mesh N. Grid refinement studies confirm that the third order accuracy in time and space for the numerical solution u^n is achieved at all grid points. We also observe that the numerical solution v^n is of the third order in time and space as well.

In [17], an immersed interface method is presented for a piecewise constant velocity. A piecewise quadratic interpolation on a cell $[x_{j-1},x_j]$ which contains a jump discontinu-

Table 1: Numerical errors in the solutions and the order of convergence of the IIM-CIP method.

Interface condition	$[u]=0$				$[cu]=0$			
N	100	200	400	800	100	200	400	800
$\epsilon(u^n)$	5.50e-2	1.03e-2	1.41e-3	1.79e-4	1.10e-1	2.07e-2	2.82e-3	3.58e-4
order		2.47	2.80	2.97		2.40	2.87	2.97
$\epsilon(v^n)$	6.13	1.10	1.57e-1	2.00e-2	12.2	2.20	3.15e-1	4.01e-2
order		2.40	2.87	2.97		2.47	2.80	2.97

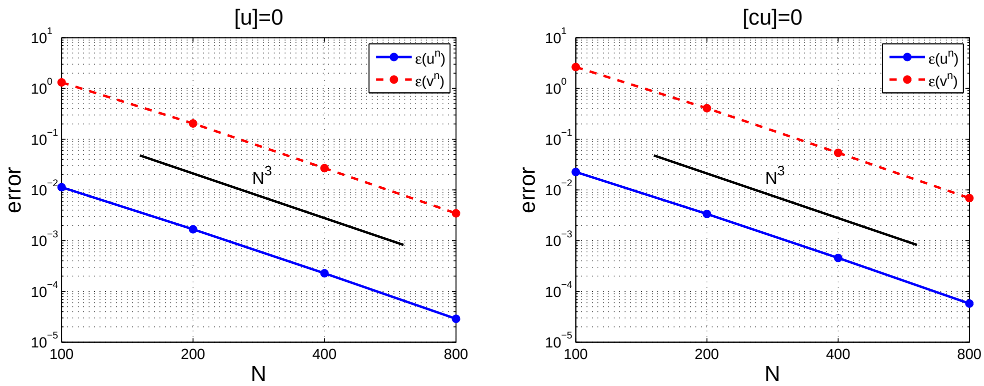

Figure 2: The third order convergence against the number of mesh N of the numerical error in the numerical solution by the IIM-CIP. The error is computed by (3.8) at $t=0.5$.

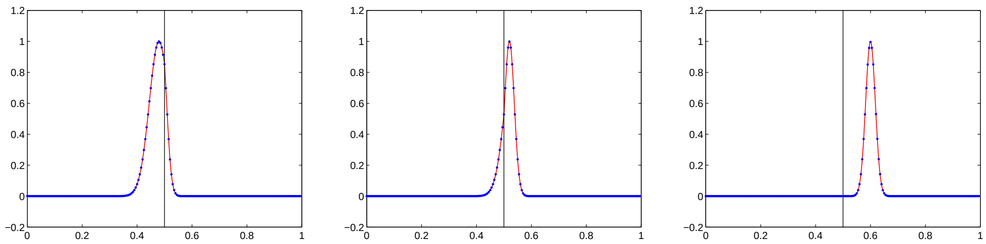

Figure 3: 1-D transport with $c_1=2$ and $c_2=1$ and jump condition $[u]=0$. The vertical solid line indicates the interface $\alpha=0.5+\frac{\sqrt{2}}{100}$. The plots are the numerical solution (dot) and the exact solution (solid) at $t=0.14$ (left), $t=0.17$ (center), $t=0.25$ (right). The mesh size is $\frac{1}{200}$.

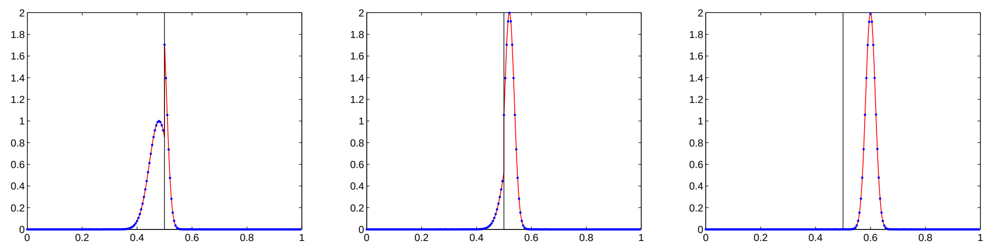

Figure 4: 1-D transport with $c_1=2$ and $c_2=1$ and jump condition $[cu]=0$. The vertical solid line indicates the interface $\alpha=0.5+\frac{\sqrt{2}}{100}$. The plots are the numerical solution (dot) and the exact solution (solid) at $t=0.14$ (left), $t=0.17$ (center), $t=0.25$ (right). The mesh size is $\frac{1}{200}$.

ity in $c(x)$ is constructed based on the immersed interface method and solution values at local three grid points. The underlined time integration method used is Lax-Wendorff method. The method causes visible oscillations in the numerical solution due to the fact that the Lax-Wendroff scheme is dispersive.

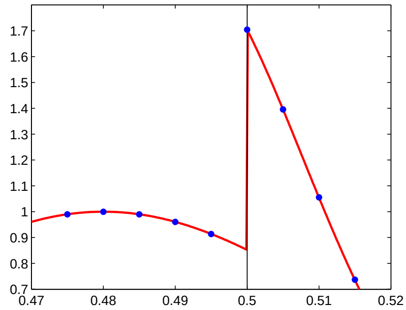

Figure 5: The plots are the numerical solution (dot) and the exact solution (solid) at $t=0.14$ around the interface $x=0.5$.

4 IIM-CIP for Maxwell's equations in one dimension

Let us consider one dimensional Maxwell's equations (1.2) for $x\in[0,1]$, $t>0$, with periodic boundary condition. We begin with the case μ and ε are constants. The solution update scheme is based on the D'Alambert formula:

$$H(t_{n+1},x)=\frac{H(t_n,x-c\Delta t)+H(t_n,x+c\Delta t)}{2}-\frac{E(t_n,x-c\Delta t)-E(t_n,x+c\Delta t)}{2c\mu},$$
$$E(t_{n+1},x)=\frac{E(t_n,x-c\Delta t)+E(t_n,x+c\Delta t)}{2}-\frac{H(t_n,x-c\Delta t)-H(t_n,x+c\Delta t)}{2c\epsilon},$$

where $c=\frac{1}{\sqrt{\mu\epsilon}}$. The formula follows from the fact that the transformations

$$u^1=\sqrt{\mu}H-\sqrt{\varepsilon}E,\quad u^2=\sqrt{\mu}H+\sqrt{\varepsilon}E,$$

satisfy the transport equations $u^1_t+cu^1_x=0$, $u^2_t-cu^2_x=0$.

Let us denote the numerical solution to $H(t_n,x_k)$, $H_x(t_n,x_k)$, $E(t_n,x_k)$ and $E_x(t_n,x_k)$ by H^n_k, $H^n_{x,k}$, E^n_k and $E^n_{x,k}$, respectively. Let $h^{k-1,k}(x)$ and $e^{k-1,k}(x)$ be the cubic polynomials on the grid $[x_{k-1},x_k]$ at time $t=t_n$ determined by the conditions

$$h^{k-1,k}(x_{k-1})=H^n_{k-1},\quad h^{k-1,k}_x(x_{k-1})=H^n_{x,k-1},\quad h^{k-1,k}(x_k)=H^n_k,\quad h^{k-1,k}_x(x_k)=H^n_{x,k},$$
$$e^{k-1,k}(x_{k-1})=E^n_{k-1},\quad e^{k-1,k}_x(x_{k-1})=E^n_{x,k-1},\quad e^{k-1,k}(x_k)=E^n_k,\quad e^{k-1,k}_x(x_k)=E^n_{x,k}.$$

Let us assume the CFL number is less or equal to 1. Then $x_k-c\Delta t\in[x_{k-1},x_k]$ and CIP scheme for Eq. (1.2) is given by

$$H^{n+1}_k=\frac{h^{k-1,k}(x_k-c\Delta t)+h^{k,k+1}(x_k+c\Delta t)}{2}-\frac{e^{k-1,k}(x_k-c\Delta t)-e^{k,k+1}(x_k+c\Delta t)}{2c\mu},$$
$$E^{n+1}_k=\frac{e^{k-1,k}(x_k-c\Delta t)+e^{k,k+1}(x_k+c\Delta t)}{2}-\frac{h^{k-1,k}(x_k-c\Delta t)-h^{k,k+1}(x_k+c\Delta t)}{2c\varepsilon},$$

and $H_{x,k}^{n+1}$ and $E_{x,k}^{n+1}$ are given by replacing the polynomials within H_k^{n+1} and E_k^{n+1} with the derivatives.

Now we consider the Maxwell's equations with ε and μ being piecewise constants, i.e., $\varepsilon=\varepsilon^-$ and $\mu=\mu^-$ in $x<\alpha$ and $\varepsilon=\varepsilon^+$ and $\mu=\mu^+$ in $\alpha<x$. The interface conditions for H and E at the interface are $[H]=0$ and $[E]=0$. The interface relations are

$$\begin{aligned}
&[H]=0, \quad \left[\frac{1}{\varepsilon}H_x\right]=0, \quad \left[\frac{1}{\mu\varepsilon}H_{xx}\right]=0, \quad \left[\frac{1}{\mu\varepsilon^2}H_{xxx}\right]=0,\\
&[E]=0, \quad \left[\frac{1}{\mu}E_x\right]=0, \quad \left[\frac{1}{\mu\varepsilon}E_{xx}\right]=0, \quad \left[\frac{1}{\mu^2\varepsilon}E_{xxx}\right]=0,
\end{aligned}$$

which are obtained in a usual manner in IIM; first differentiating the relation $[H]=0$ with respect to t, then substituting the equation $\mu H_t=E_x$ to get $\left[\frac{1}{\mu}E_x\right]=0$. Differentiate this relation again with respect to t and substitute $\varepsilon E_t=H_x$, we obtain $\left[\frac{1}{\mu\varepsilon}H_x\right]=0$. The others are given by repeating this procedure.

Let us assume that the interface $x=\alpha$ is included in $[x_{j-1},x_j]$. Let us denote the immersed interface cubic profiles for H and E on the cell $[x_{j-1},x_j]$ by $h^\pm(x)$ and $e^\pm(x)$ respectively. From the interface relations,

$$\begin{aligned}
h^\pm(x)&=a_0+\varepsilon^\pm a_1\frac{x-\alpha}{\Delta x}+(\mu\varepsilon)^\pm\frac{a_2}{2}\left(\frac{x-\alpha}{\Delta x}\right)^2+(\mu\varepsilon^2)^\pm\frac{a_3}{3!}\left(\frac{x-\alpha}{\Delta x}\right)^3,\\
e^\pm(x)&=b_0+\mu^\pm b_1\frac{x-\alpha}{\Delta x}+(\mu\varepsilon)^\pm\frac{b_2}{2}\left(\frac{x-\alpha}{\Delta x}\right)^2+(\mu^2\varepsilon)^\pm\frac{b_3}{3!}\left(\frac{x-\alpha}{\Delta x}\right)^3.
\end{aligned}$$

The coefficients a and b are determined by the interpolation condition at two end points x_{j-1}, x_j, i.e.,

$$A(\epsilon,\mu)a=(H_j^n,\Delta x H_{x,j}^n,H_{j-1}^n,\Delta x H_{x,j-1}^n)^\top, \quad A(\mu,\epsilon)b=(E_j^n,\Delta x E_{x,j}^n,E_{j-1}^n,\Delta x E_{x,j-1}^n)^\top,$$

where

$$A(\epsilon,\mu)=\begin{pmatrix}
1 & \varepsilon^+\theta & \frac{(\mu\varepsilon)^+\theta^2}{2} & \frac{(\mu\varepsilon^2)^+\theta^3}{3!}\\
0 & \varepsilon^+ & (\mu\varepsilon)^+\theta & \frac{(\mu\varepsilon^2)^+\theta^2}{2}\\
1 & \varepsilon^-(\theta-1) & \frac{(\mu\varepsilon)^-(\theta-1)^2}{2} & \frac{(\mu\varepsilon^2)^-(\theta-1)^3}{3!}\\
0 & \varepsilon^- & (\mu\varepsilon)^-(\theta-1) & \frac{(\mu\varepsilon^2)^-(\theta-1)^2}{2}
\end{pmatrix}, \quad \theta=\frac{x_j-\alpha}{\Delta x}.$$

The numerical solutions H_j^{n+1} and E_j^{n+1} at the irregular point x_j are then given by

$$\begin{aligned}
H_j^{n+1}&=\frac{h^+(x_j-c^+\Delta t)+h^{j,j+1}(x_j+c^+\Delta t)}{2}-\frac{e^+(x_j-c^+\Delta t)-e^{j,j+1}(x_j+c^+\Delta t)}{2c^+\mu^+},\\
E_j^{n+1}&=\frac{e^+(x_j-c^+\Delta t)+e^{j,j+1}(x_j+c^+\Delta t)}{2}-\frac{h^+(x_j-c^+\Delta t)-h^{j,j+1}(x_j+c^+\Delta t)}{2c^+\varepsilon^+},
\end{aligned}$$

where $c^+ = \left(\sqrt{\mu^+\epsilon^+}\right)^{-1}$. $H_{x,j}^{n+1}$ and $E_{x,j}^{n+1}$ are given by replacing the polynomials within H_j^{n+1} and E_j^{n+1} with the derivatives. We note that the point x_{j-1} is also an irregular point, and the immersed interface cubic profiles are used to update the numerical solutions at this point. For instance, H_{j-1}^{n+1} is given as

$$H_{j-1}^{n+1} = \frac{h^{j-2,j-1}(x_{j-1}-c^-\Delta t)+h^-(x_{j-1}+c^-\Delta t)}{2} - \frac{e^{j-2,j-1}(x_{j-1}-c^-\Delta t)-e^-(x_{j-1}+c^-\Delta t)}{2c^-\mu^-},$$

where $c^- = \left(\sqrt{\mu^-\epsilon^-}\right)^{-1}$.

We investigate the performance of the IIM-CIP for the Maxwell's equations. Consider the Maxwell's equations (1.2) with

$$\varepsilon(x) = \begin{cases} \varepsilon^- = 1, & 0 \le x \le \alpha, \\ \varepsilon^+ = \frac{4}{3}, & \alpha \le x \le 1. \end{cases}, \qquad \mu(x) = \begin{cases} \mu^- = 1, & 0 \le x \le \alpha, \\ \mu^+ = 3, & \alpha \le x \le 1. \end{cases}$$

where $\alpha = 0.5 + \frac{\Delta x}{2}$. The spatial domain $[0,1]$ is uniformly discretized with mesh size $\Delta x = \frac{1}{400}$, and the time step size is $\Delta t = \Delta x$. The E field is excited at $x = 0$ by the sine and square wave pulse

$$f(t) = \sin\left(\frac{2\pi t}{40\Delta x}\right) \quad (0 \le t \le 0.1), \quad f(t) = 1 \quad (0.2 \le t \le 0.3), \quad f(t) = 0 \quad \text{otherwise.}$$

The wave speed $c = \frac{1}{\sqrt{\varepsilon\mu}}$ takes 1 in $x \le \alpha$ and 0.5 in $\alpha \le x$. On the left of the interface, the medium is vacuum, and the medium on the right is a dielectric with $\varepsilon^+ = \frac{4}{3}, \mu^+ = 3$. The impedances of the media are $Z_1 = 1$ on the left and $Z_2 = \frac{3}{2}$ on the right. Since the amplitudes of the generated fields H and E are 0.5, the amplitudes of the reflective and the transmitted field E will be $\frac{Z_2 - Z_1}{Z_2 + Z_1} 0.5 = 0.1$ and $\frac{2Z_2}{Z_2 + Z_1} 0.5 = 0.6$, respectively, and those of H field will be $\frac{Z_2 - Z_1}{Z_1(Z_2 + Z_1)} 0.5 = 0.1$ and $\frac{2}{Z_2 + Z_1} 0.5 = 0.4$, respectively.

The numerical results are shown in Fig. 6. The numerical solutions to $H(t,x)$ (left column) and $E(t,x)$ (right column) at time $t = 0.15$, $t = 0.65$ and $t = 1$ are depicted. There are no significant oscillations observed in the vicinity of the interface, and the magnitudes of the computed solution are all almost coincide with the exact ones.

5 Conclusion

We have proposed a numerical scheme for one-dimensional hyperbolic equations in discontinuous medias. We showed that the immersed interface cubic profile maintains the accuracy of the solution at the interface.

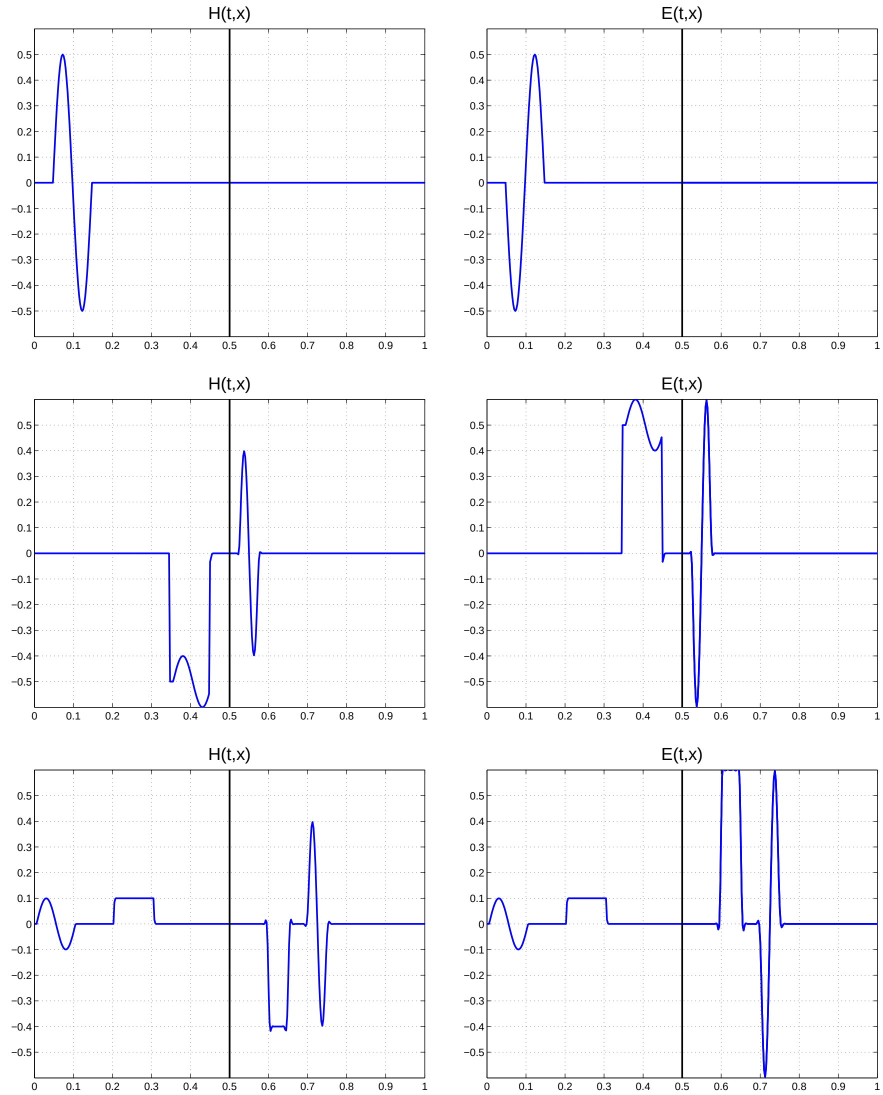

Figure 6: 1-D Maxwell's equations with $\mu^- = \varepsilon^- = 1$ $(x < 0.5 + \frac{\Delta x}{2})$and $\mu^+ = 3$, $\varepsilon^+ = \frac{4}{3}$ $(0.5 + \frac{\Delta x}{2} \leq x)$. The interface condition $[H] = [E] = 0$ is imposed at the interface $x = 0.5 + \frac{\Delta x}{2}$ (vertical line). The left plots are snap shots of the numerical solutions to H at $t = 0.15, t = 0.65$ and $t = 1$. The right plots are the numerical solution to E at the same time. The mesh size is $\frac{1}{400}$.

Acknowledgments

This research is supported by the Aihara Project, the FIRST program from JSPS, initiated by CSTP. The research of K. Ito was partially supported by the Army Research Office under DAAD19-02-1-0394, US-ARO grant 49308-MA, and US-AFSOR grant FA9550-06-1-0241.

References

[1] R. P. Agarwal, Sharp Hermite interpolation error bounds for derivatives, Nonlinear Analysis, 17 (1991), 773-786.
[2] T. Aoki, Interpolated differential operator (IDO) scheme for solving partial differential equations, Computer Physics Communications, 102 (1997), 132-146.
[3] D. Barada, T. Fukuda, M. Itoh, and T. Yatagai, Cubic interpolated propagation scheme in numerical analysis of lightwave and optical force, Opt. Express, 14 (2006), 4151-4168.
[4] L. C. Evans, Partial differential equations, vol. 19 of Graduate Studies in Mathematics, American Mathematical Society, Providence, RI, 1998.
[5] Y. Imai and T. Aoki, A higher-order implicit IDO scheme and its CFD application to local mesh refinement method, Computational Mechanics, 38 (2006), 211-221.
[6] R. J. LeVeque and Z. Li, The immersed interface method for elliptic equations with discontinuous coefficients and singular sources, SIAM J. Numer. Anal., 31 (1994), 1019-1044.
[7] Z. Li and K. Ito, The immersed interface method, Society for Industrial and Applied Mathematics (SIAM), Philadelphia, PA, 2006.
[8] Y. Ogata, T. Yabe, and K. Odagaki, An accurate numerical scheme for Maxwell equation with CIP-method of characteristics, Commun. Comput. Phys., 1 (2006), 311-335.
[9] J. C. Strikwerda, Finite difference schemes and partial differential equations, The Wadsworth, Pacific Grove, CA, 1989.
[10] H. Takewaki, A. Nishiguchi, and T. Yabe, Cubic interpolated pseudo-particle method (CIP) for solving hyperbolic-type equations, J. Comput. Phys., 61 (1985), 261-268.
[11] T. Utsumi, T. Kunugi, and T. Aoki, Stability and accuracy of the cubic interpolated propagation scheme, Computer Physics Communications, 101 (1997), 9-20.
[12] T. Yabe, A universal cubic interpolation solver for compressible and incompressible fluids, Shock Waves, 1 (1991), 187-195.
[13] T. Yabe and T. Aoki, A universal solver for hyperbolic equations by cubic-polynomial interpolation. I. One-dimensional solver, Comput. Phys. Comm., 66 (1991), 219-232.
[14] T. Yabe, T. Ishikawa, P. Y. Wang, T. Aoki, Y. Kadota, and F. Ikeda, A universal solver for hyperbolic equations by cubic-polynomial interpolation. II. Two- and three-dimensional solvers, Comput. Phys. Comm., 66 (1991), 233-242.
[15] T. Yabe, H. Mizoe, K. Takizawa, H. Moriki, H. N. Im, and Y. Ogata, Higher-order schemes with CIP method and adaptive Soroban grid towards mesh-free scheme, J. Comput. Phys., 194 (2004), 57-77.
[16] T. Yabe, F. Xiao, and T. Utsumi, The constrained interpolation profile method for multiphase analysis, J. Comput. Phys., 169 (2001), 556-593.
[17] C. Zhang and R. J. LeVeque, The immersed interface method for acoustic wave equations with discontinuous coefficients, Wave Motion, 25 (1997), 237-263.